

Segmentation Analysis for Brain Stroke Diagnosis Based on Susceptibility-Weighted Imaging (SWI) using Machine Learning

Shaarmila Kandaya¹, Abdul Rahim Abdullah², Norhashimah Mohd Saad³, Ezreen Farina⁴, Ahmad Sobri Muda⁵

Department Electrical Engineering, Universiti Teknikal Malaysia Melaka, Malaysia^{1, 2, 4}

Department of Electrical and Electronic Engineering Technology, Universiti Teknikal Malaysia Melaka, Malaysia³

Faculty of Medicine and Health Sciences, Universiti Putra Malaysia, 43400 Serdang, Selangor, Malaysia⁵

Abstract—Magnetic Resonance Imaging (MRI) plays a crucial role in diagnosing brain disorders, with stroke being a significant category among them. Recent studies emphasize the importance of swift treatment for stroke, known as "time is brain," as early intervention within six hours of stroke onset can save lives and improve outcomes. However, the conventional manual diagnosis of brain stroke by neuroradiologists is subjective and time-consuming. To address this issue, this study presents an automatic technique for diagnosing and segmenting brain stroke from MRI images according to pre and post stroke patient. The technique utilizes machine learning methods, focusing on Susceptibility Weighted Imaging (SWI) sequences. The machine learning technique involves four stages, those are pre-processing, segmentation, feature extraction, and classification. In this paper, pre-processing and segmentation are proposed to identify the stroke region. The segmentation performance is assessed using Jaccard indices, Dice Coefficient, false positive, and false negative rates. The results show that adaptive threshold performs best for stroke lesion segmentation, with good improvement stroke patient that achieving the highest Dice coefficient of 0.96. In conclusion, this proposed stroke segmentation technique has promising potential for diagnosing early brain stroke, providing an efficient and automated approach to aid medical professionals in timely and accurate diagnoses.

Keywords—Magnetic Resonance Imaging (MRI) diagnosis, time is brain, Susceptibility Weighted Imaging (SWI) and dice coefficient

I. INTRODUCTION

Cerebrovascular accident (CVA) or stroke stands as the third leading cause of death in Malaysia [1]. This presents a significant challenge to the Malaysian healthcare system, witnessing over 50,000 new cases annually, resulting in at least 32 daily fatalities. In 2016, the government committed RM180 million to address this issue. Globally, stroke is the second leading cause of death, surpassed only by coronary artery disease, and it ranks prominently in causing long-term disability. The Malaysian National Stroke Association (NASAM) underscores the urgency of immediate medical attention for stroke, as swift treatment, especially within six hours, has been shown to save lives. However, the scarcity of neuroradiologists, with only 107 specialists, and the reliance on manual interpretation of magnetic resonance imaging (MRI) images hinder timely treatment efforts.

Brain stroke, characterized by a network of small blood vessels facilitating blood flow through a stroke or blocked artery, requires rapid and accurate diagnosis for prompt intervention. While MRI has gained preference over conventional angiography for diagnosing brain stroke, the current practice involves labor-intensive visual inspection, delaying the process [2]. Timely diagnosis and treatment are critical to preventing disability caused by insufficient blood and oxygen, leading to nerve cell death. Diagnostic considerations include factors like infarct volume, penumbra size, and the presence of adequate early stroke, all crucial for successful treatment [3]. Neuroradiologists urgently need efficient tools for quick and accurate acute stroke diagnosis.

Moreover, brain stroke detection from MRI images faces challenges due to noise, artifacts, vessel size, and structural heterogeneity [4]. Novel methods for segmenting and classifying medical images are regularly proposed [5]. Common machine learning techniques for vessel segmentation, such as region growing, clustering, and active contours, face limitations related to sensitivity to noise and segmentation issues [6]. The manual segmentation by neuroradiologists, though time-consuming, highlights the importance of processing time speed and accuracy in computer-aided diagnostic systems [7].

Traditional machine learning methods, while effective, require complex denoising and feature extraction before classification, leading to prolonged computation times [8]. Recent studies acknowledge the robustness of machine learning in processing noisy medical images, yet the challenges of long computation times persist [9]. As a solution, hybrid frameworks incorporating machine learning techniques are considered promising for achieving optimal accuracy in early stroke classification.

This review explores the significance of stroke, brain stroke concepts, and MRI in the context of the human brain. Stroke, or cerebral infarction, ranks as the third leading cause of death and the primary cause of permanent disability in Malaysia [10]. The profound public health impact is evident in high initial treatment, rehabilitation, and chronic care costs. The urgency of stroke is highlighted by its occurrence every 45 seconds in the United States, affecting 795,000 individuals annually. The devastating impact on neurons and synapses during a stroke, leading to accelerated aging of the ischemic brain, underscores

the critical notion that "time is the brain." Despite this urgency, there is a notable absence of computer-aided diagnosis (CAD) systems tailored for stroke, unlike those available for fields like mammography and breast imaging. Existing studies on CAD systems and methodologies emphasize their potential to enhance diagnostic precision for radiologists [11].

II. LITERATURE REVIEW

A. Human Brain

The human brain stands out as one of the most intricate organs in the human body, comprising billions of interconnected nerve cells forming complex networks. Its spatiotemporal patterns contribute to its recognition as the most intricate system, wherein the alignment between structural and functional connections relies on spatial resolution and temporal scale [7]. Endowed with the capacity to govern intelligence, creativity, emotions, and memory, the brain is shielded by the skull and comprises the cerebrum, cerebellum, and brainstem, as illustrated in Fig. 1. Further division into lobes reveals specific responsibilities:

- 1) The frontal lobe manages problem-solving, decision-making, and motor skills.
- 2) The parietal lobe oversees sensation, handwriting, and posture.
- 3) The temporal lobe plays a role in memory and hearing.
- 4) The occipital lobe houses the brain's visual processing system.

Facilitating communication with the body, the brain utilizes 12 pairs of cerebrovascular vessels through the spinal cord and blood flow. Among these, ten pairs originating in the brainstem control functions like hearing, eye movements, facial sensations, taste, swallowing, and muscle movements in the face, neck, shoulders, and tongue. Meanwhile, cerebral blood vessels governing smell and vision originate in the cerebrum. Hence, maintaining proper blood circulation in vessels is crucial to prevent neuropathy, which could lead to nerve cell damage and subsequent cell death [8]. Refer to Fig. 1, for a visual representation of the human brain's anatomy.

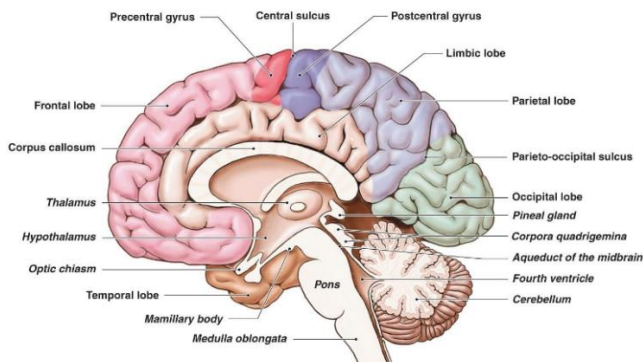


Fig. 1. Anatomy of human brain.

B. Brain Stroke Diagnosis

In this universe, second-leading cause of death is stroke, demanding prompt intervention to prevent severe long-term disability or fatality. This occurs when a blood clot obstructs a blood vessel or ruptures, impeding blood flow to a specific

brain region. The classification, depicted in Fig. 2, distinguishes between ischemic stroke, where a blood vessel abruptly obstructs a brain artery [1], and hemorrhagic stroke (cerebral hemorrhage), characterized by the rupture of a blood vessel [2].

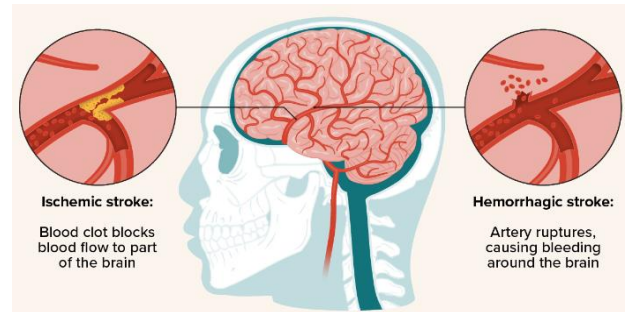


Fig. 2. Types of stroke.

Stroke exerts a significant impact on public health, resulting in substantial expenditures for primary care, rehabilitation, and the management of chronic conditions. In 2015, stroke accounted for 6.3 million deaths globally, ranking as the second leading cause of death after ischemic heart disease. Despite its persistent status as the third leading cause of death in Malaysia as reported by the Institute for Health Metrics and Evaluation in June 2019, there is a notable absence of computer-aided diagnosis (CAD) systems designed specifically for stroke, unlike the numerous CAD systems available for fields such as mammography and thorax. Research on CAD systems and techniques underscores the potential for enhancing the diagnostic accuracy of radiologists.

Reperfusion injury plays a pivotal role in the outcomes of ischemic stroke patients upon the restoration of blood flow [3]. Various approaches, including ischemic preconditioning, preconditioning, and postconditioning, have been explored for cardio protection, yielding diverse results regarding potential treatments [4]. The timely reinstatement of local blood flow is crucial for salvaging threatened tissue, minimizing cell death, and ultimately reducing patient disability. Successful recanalization significantly increases the likelihood of a favorable outcome, with a fourfold reduction in mortality compared to patients without recanalization [5]. Strategies for recanalization involve thrombolytic drugs such as tissue plasminogen activator (tPA) and/or mechanical interventions like thrombectomy using distal or proximal devices. Thrombectomy, involving the removal of blood clots through a catheter with an attached mechanical device, is particularly attractive due to its short intervention time, high recanalization rates, and potential for efficient blood flow restoration. However, the associated risks necessitate careful consideration, and the procedure should be reserved for patients meeting specific criteria, including a large circumference, small infarct, and good collateral circulation. In essence, precise patient selection based on pre-treatment imaging is crucial for achieving favorable outcomes with mechanical recanalization [6].

C. Magnetic Resonance Imaging (MRI)

Magnetic Resonance Imaging (MRI) is a medical imaging technique that uses strong magnetic fields and radio waves to

generate detailed images of the body's internal structures. MRI is commonly used in the early diagnosis of strokes and plays a crucial role in assessing the extent and location of the stroke, determining the appropriate treatment, and monitoring the patient's progress. When it comes to early stroke diagnosis, MRI provides several advantages over other imaging techniques. Here's how it works:-

1) *Visualization of brain anatomy:* MRI produces high-resolution images that can accurately depict the brain's anatomy, allowing healthcare professionals to identify any abnormalities or changes associated with a stroke. It provides detailed information about the brain's structure, including differentiating between gray and white matter, which is essential for detecting ischemic (clot-based) or hemorrhagic (bleeding-based) strokes.

2) *Differentiating stroke types:* MRI can help differentiate between ischemic and hemorrhagic strokes, which is crucial for determining the appropriate treatment approach. Ischemic strokes occur due to a blockage in a blood vessel, while hemorrhagic strokes result from bleeding in the brain. By examining the MRI images, doctors can identify the type and location of the stroke.

3) *Time-sensitive techniques:* Certain MRI techniques are time-sensitive and can detect changes in brain tissue that occur shortly after a stroke. Susceptibility-Weighted Imaging (SWI) is particularly useful in the early stages of stroke diagnosis. It measures the movement of water molecules in the brain and can detect restricted diffusion in areas affected by an ischemic stroke within minutes of onset. This early identification helps guide treatment decisions promptly.

4) *Assessment of perfusion:* Perfusion-weighted imaging (PWI) is another MRI technique that provides information about blood flow to the brain. PWI helps assess the extent of damaged brain tissue and determine the viability of the surrounding areas. By comparing SWI and PWI, healthcare professionals can identify the ischemic penumbra, which refers to the region around the stroke where brain tissue is at risk but still salvageable. This information aids in treatment planning.

5) *Detection of complications:* MRI can also identify complications associated with strokes, such as swelling, edema, or the presence of blood in the brain. These factors are crucial in determining the severity of the stroke, guiding treatment decisions, and assessing the patient's prognosis.

Overall, MRI is a valuable tool in the early diagnosis of brain strokes. Its ability to provide detailed images of the brain's anatomy, differentiate between stroke types, detect early changes in brain tissue, assess perfusion, and identify complications makes it an essential imaging technique in stroke management. It enables healthcare professionals to make informed decisions regarding treatment options and improve patient outcomes.

Two types of stroke, namely hemorrhagic and ischemic, are distinguished based on interpretation [12]. Ischemic strokes constitute approximately 70% of all cases, presenting with neurological deficits that endure for more than 24 hours or result in death within that timeframe [13]. Hemorrhagic

strokes, accounting for about 12% of all strokes, are further divided into 9% intracerebral hemorrhages and 3% subarachnoid hemorrhages. Hemorrhagic strokes occur due to the rupture of a cerebral blood vessel or an abnormality in a blood vessel, causing bleeding into adjacent brain tissue. This leads to impairment of brain function and often results in death rather than permanent disability. In contrast, ischemic strokes, caused by the blockage of blood vessels supplying the brain, are more prevalent.

Within the Oxfordshire Community Stroke Project [14], instances of stroke are categorized into four groups by considering the initial symptoms and their severity. This classification aims to anticipate the extent of the stroke, the affected brain regions, underlying causes, and the prognosis. The four groups include total anterior circulation stroke syndrome (TACS), partial anterior circulation stroke syndrome (PACS), lacunar stroke syndrome (LACS), and posterior circulation stroke syndrome (POCS). The most common type of LACS is caused by blockage of small arteries that supply deep brain structures. Patients usually suffer from pure motor or sensory deficits, sensorimotor deficits, or ataxic hemiplegia [15]. TACS occurs when the blood supply to the anterior and middle cerebral arteries on both sides of the brain is compromised, causing hemiplegia. PACS is a less severe form of TACS that exhibits some, but not all, of the symptoms associated with TACS. POCS is caused by a reduced blood supply to the posterior cerebral artery on one side of the brain [16]. Fig. 3 shows the MRI machine used for scanning.



Fig. 3. MRI machine used for scanning.

III. METHODOLOGY

The flowchart for MRI image analysis using machine learning is shown in Fig. 4. All techniques, including image pre-processing, picture segmentation and features extraction are included in the flow chart.

A. Pre-processing Stage (Normalization, Background Removal and Enhancement)

Suitable pre-processing will be identified to enhance and remove the noise. Image normalization, background removal and enhancement will be included (Shakunthala and Helenprabha, 2019). Mathematical methods known as "image enhancement techniques" are designed to increase the quality of a particular image, either for usage by a human viewer or for computer processing.

The kind of intensity depth must be transformed to double precision throughout the normalisation process, with the minimum value set to "0" and the maximum value set to "1". To make the computation of the algorithm simpler, this

procedure is necessary. Eq. (1), where N is the bit depth applied to the normalisation computation, states the equation.

$$I(x, y)_{normalization} = \frac{I(x, y)}{2^N - 1}, N = bits \quad (1)$$

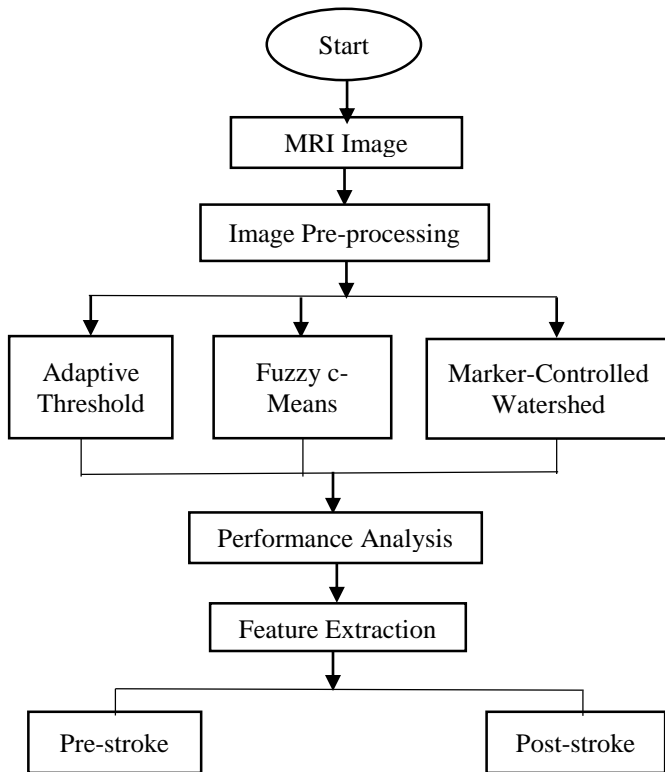


Fig. 4. Flow chart of MRI image analysis using machine learning technique.

Background pixels in MRI images need to be eliminated. This is due to the fact that specific brain structures and the background have similar intensities. Adaptive thresholding and morphological techniques can be used to achieve this. The threshold version's binary image output is its ultimate product. In order to trace the closed regions and their boundaries of connected neighbourhoods, boundary extraction algorithms are required. Enhancement techniques can be used to expand the intensity and improve the contrast. Several techniques can be implemented such as gamma-law and contrast stretching algorithms.

B. Segmentation using Machine Learning Techniques

Image segmentation is crucial because radiologists need to know the accurate location, size, intensity and other lesion's details to make a conclusion or diagnosis. The segmentation involves detecting and labelling meaningful regions in the given image data. Three types of image segmentation technique will be analyzed which are Adaptive Threshold, Fuzzy C-Means and Marker-Controlled Watershed.

1) *Adaptive threshold*: An adaptive threshold is a segmentation technique that creates a binary picture from a grayscale image of a fixed value. Thresholding is the technique of converting a grayscale image into a black and white image by turning all of the pixels to either white or black depending

on whether their value is above or below a specified threshold [17]. Eq. (2) illustrates adaptive threshold, which determines each pixel's threshold value by referring to the gray-level intensity of its neighbours.

$$G(x, y) = \begin{cases} 1 & \text{if } I(x, y) \geq \tau \\ 0 & \text{otherwise} \end{cases} \quad (2)$$

2) *Fuzzy C-Means*: Fuzzy C-Means (FCM) is one of the popular algorithm in clustering [18]. Data that belong to two or more clusters with various membership coefficients can be processed iteratively in this way. After creating the initial fuzzy partition matrix, the initial fuzzy cluster centres are computed. In order to determine where the clusters should be placed, the objective function is minimised while the cluster centres and membership grade point are updated at each iteration's step. When the maximum number of iterations is reached or when the improvement in the objective function between two successive iterations is less than the minimum amount of improvement required, the procedure comes to an end [19].

The iteration of FCM is performed through two parameters, namely the membership degree and the center of the cluster. When the repeated steps come to an end or reach their maximum number of iterations, these parameters are altered [20]. Additionally, when the objective function improvements of two successive iterations are less than the minimum amount of improvement set, the change of these parameters is affected. The low, medium, and high clusters are the starting points for the Fuzzy C-Means technique used in this segmentation [21]. The centre of each cluster will be used to determine the data point. The cluster's data points should all equal one. The algorithm relies on minimising the objective function presented below.

$$J_m = \sum_{i=1}^N \sum_{j=1}^C u_{ij}^m \|x_i - c_j\|^2, 1 \leq m \leq \infty \quad (3)$$

where, u_{ij} represents the membership degree of data point x_i in cluster j , where x_i is the d -dimensional center of the i th cluster, c_j is the d -dimensional center of the cluster, and $\|*\|$ is a norm indicating the similarity between measured data and the center. The term M , referred to as the fuzziness exponent, is any number greater than 1.

3) *Marker-Controlled watershed*: A gradient-based segmentation method is called watershed segmentation. According to this study's findings, the watershed segmentation identifies the water basins and watershed ridge lines by classifying each pixel's intensity as either high intensity or low intensity on a surface [22]. The gradient magnitude is calculated using the image foreground and background markers and the edge detection technique. The watershed ridge line and morphological operation are then used [23]. Based on the provided watershed ridge lines, the watershed transform is created. The input image $I(x, y)$ and the gradient along x and y -axis are calculated according to Eq. (4).

$$I_x = \frac{\partial f}{\partial x} = (z_7 + 2z_8 + z_9) - (z_1 + 2z_2 + z_3) \quad (4)$$

$$I_y = \frac{\partial f}{\partial y} = (z_3 + 2z_6 + z_9) - (z_1 + 2z_4 + z_7)$$

Then the gradient of the image is defined as:

$$\nabla I(x, y) = \frac{\partial f}{\partial x} i + \frac{\partial f}{\partial y} j = I_x i + I_y j \quad (5)$$

where, i and j are unit vectors along x and y axis respectively. The magnitude of gradient is given by:

$$g(x, y) = |\nabla f(x, y)| = \sqrt{g_x^2 + g_y^2} \quad (6)$$

The image may have an excessive amount of gradient segmentation as a result of noise and other irregularities [24]. Thus to overcome the problem, morphological operation technique can be implemented.

C. Features Extraction

A collection of features are extracted from each image based on the segmentation technique. Meaningful characteristics must be developed before they can be used as input in the classification process [25]. These properties may be based on spectral, textural, or statistical examination of an image's grey level. To complete the diagnosis, other general features like signal intensity are needed [26]. All the features that radiologists discovered when examining the brain scans are listed in Table IV. Table I provides a list of the feature extractions that reflect nearby stroke area regions.

TABLE I. LIST OF FEATURES EXTRACTION RESULTS AND DISCUSSIONS

(a) Medical diagnosis	(b) Features extracted
<u>Structural elements:</u> -	<u>Statistical features in spatial domain:</u> -
1. Number of lesions	1. Intensity
2. Shape	2. Mean
3. Location	3. Median
4. Elements within the lesion	4. Standard deviation
5. Internal and external capsules	5. Perimeter
6. Midline shift, distended and swell	6. Gradient value
7. Symmetric	7. Entropy
<u>Lesion's characteristics:</u> -	8. skewness
8. Intensity	9. Euclidian distance
9. Region's area	10. Texture analysis
10. Region's diameter	<u>Shape, boundary, contour, location:</u> -
11. Mean	11. Area
12. Standard deviation	12. Perimeter
13. Compactness	13. Compactness
14. Density	14. Mean of region boundary
15. Volume	15. Volume
16. Contrast	16. Density
	17. Invariant and boundary moment

A. Performance Evaluation

The segmentation results obtained from the proposed technique will be compared with the manual reference

segmentation performed by neuroradiologists. Similarity indices based on Jaccard's and then the accuracy is obtained by finding the percentage of the number of correctly classified samples. Dice will be calculated to measure the accuracy of the segmentation for the pair of segmented and reference image.

IV. RESULTS AND DISCUSSIONS

A. Image Pre-processing

Fig. 5 displays an image portraying a stroke brain lesion characterized by hyperintensity. The maximum pixel intensity in the image is 205, and the pixels are in a 9-bit format. Based on analysis, the image underwent preprocessing using three methods: normalization, background removal, and enhancement through power-law transformation.

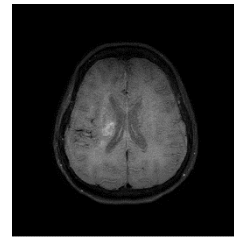


Fig. 5. Original image.

In Fig. 6, the image has undergone normalization to a 10-bit format, along with its corresponding histogram. The highest normalized intensity is recorded as 0.76908. Following the normalization process, a background removal procedure is employed to eliminate pixels, enhancing the clarity of the lesion in the image.

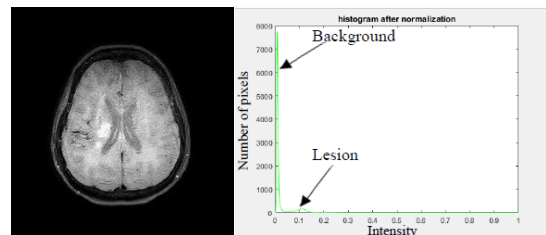


Fig. 6. Image normalization with its histogram.

In Fig. 7, background pixels have been eliminated through thresholding at 0.0563, with the highest peak observed at an intensity level of 0.1196.

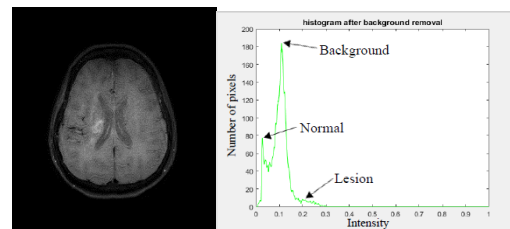


Fig. 7. Image background removal with its histogram.

Fig. 8 illustrates the result following the implementation of a power-law transformation. The peak intensity is situated at 0.6892. Analyzing the histogram, it is evident that the power-law transformation has elevated the normalized intensity to 0.3556. Simultaneously, the lesion has expanded to an intensity

level of 0.8, as indicated by arrows. The maximum intensity achieved through the gamma-law transformation is 0.7901.

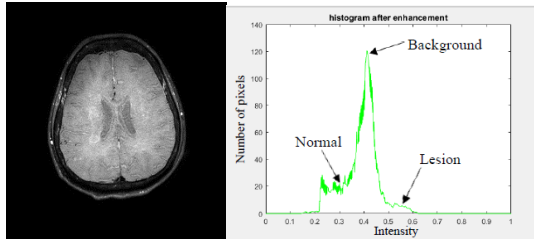


Fig. 8. Image enhancement with its histogram.

B. Image Segmentation

An automated segmentation method has been devised for segmenting Regions of Interest (ROIs) within SWI images, utilizing adaptive threshold, marker-controlled watershed with correlation template, and FCM with active contour. Each segmentation outcome is subsequently compared with a manual reference. This process pertains to the segmentation of both hyperintense and hypointense lesions in SWI images.

1) Adaptive Threshold

TABLE II. THE SEGMENTATION RESULTS OF THE SWI STROKE LESION FROM THE ORIGINAL IMAGE USING ADAPTIVE THRESHOLD SEGMENTATION TECHNIQUE

Type of Stroke patient	Pre/ Post Stroke	SWI Original Image	Brain Segmentation	Segmented Lesion Area
Poor Improvement Patient	Pre Stroke			
	Post Stroke			
Moderate Improvement Patient	Pre Stroke			
	Post Stroke			
Good Improvement Patient	Pre Stroke			
	Post Stroke			

According to the data presented in Table II, the segmentation outcomes indicate that the adaptive threshold technique is effective in delineating hyperintense lesions. However, it faces challenges in segmenting hypointense lesions due to the presence of shadow pixels, which are uncertain with the assigned threshold value from this segmentation method. The technique struggles to segment overlapping pixels resulting from noise or intensity variation in the SWI image.

2) Fuzzy c-means (FCM) with active contour: FCM is a clustering method designed to group objects with similar characteristics. This technique is combined with active contour to eliminate CSF regions by establishing boundaries within the SWI image. Computer-generated curves are employed to identify and pinpoint the Regions of Interest (ROIs). The segmentation outcomes for the stroke lesion from the original image are presented in Table III.

TABLE III. THE SEGMENTATION RESULTS OF THE SWI STROKE LESION FROM THE ORIGINAL IMAGE USING FCM WITH ACTIVE CONTOUR SEGMENTATION TECHNIQUE

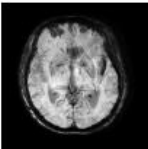
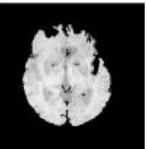
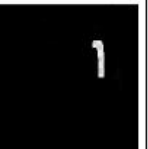
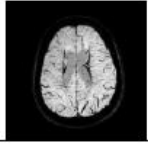








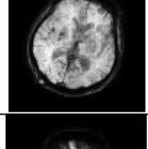


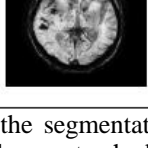
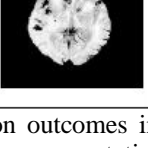
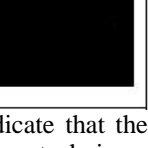
Type of Stroke patient	Pre/ Post Stroke	SWI Original Image	Brain Segmentation	Segmented Lesion Area
Poor Improvement Patient	Pre Stroke			
	Post Stroke			
Moderate Improvement Patient	Pre Stroke			
	Post Stroke			
Good Improvement Patient	Pre Stroke			
	Post Stroke			

According to Table III, the segmentation outcomes reveal that the FCM segmentation method, when combined with active contour, yields favorable results for both hyperintense

and hypointense lesions in the Regions of Interest (ROIs). However, in FCM, the presence of noise in SWI isn't factored in, making the technique susceptible to noise. To address this issue, additional refinement is applied using active contour segmentation to eliminate cerebrospinal fluid (CSF) and small pixels.

3) *Marker-controlled watershed*: Marker-controlled watershed segmentation is a segmentation method based on gradients. It is combined with a correlation template that utilizes a matching template to eliminate the cerebrospinal fluid (CSF) region in severe stroke cases. The segmentation outcomes for the stroke lesion from the original image are illustrated in Table IV.

TABLE IV. THE SEGMENTATION RESULTS OF THE SWI STROKE LESION FROM THE ORIGINAL IMAGE USING MARKER-CONTROLLED WATERSHED WITH CORRELATION TEMPLATE SEGMENTATION TECHNIQUE

Type of Stroke patient	Pre/ Post Stroke	SWI Original Image	Brain Segmentation	Segmented Lesion Area
Poor Improvement Patient	Pre Stroke			
	Post Stroke			
Moderate Improvement Patient	Pre Stroke			
	Post Stroke			
Good Improvement Patient	Pre Stroke			
	Post Stroke			

In Table IV, the segmentation outcomes indicate that the marker-controlled watershed segmentation technique, combined with the correlation template, effectively delineates Regions of Interest (ROIs) for both hyperintense and hypointense lesions. The marker-controlled watershed technique segments the ROI by utilizing the boundary formed through the watershed technique, which is based on the

gradient surface in the SWI image. To address the issue of over-segmentation resulting from the marker-controlled watershed technique, the correlation template method is introduced. This refinement aids in removing cerebrospinal fluid (CSF) and producing a more reasonable segmentation that accurately reflects the layout of the ROI.

C. Performance Evaluation for Segmentation Method

This part discusses the performance analysis and evaluation of the proposed segmentation technique. The evaluation is grounded in the analysis of 24 samples, specifically focusing on the optimal appearance of SWI lesions. The evaluation centers on stroke lesions, encompassing 18 samples from stable stroke patients and six from patients with more severe conditions. Performance evaluation employs metrics including the Jaccard index (area overlap, AO), Dice coefficient (DC), false positive rate (FPR), and false negative rate (FNR). A higher index signifies greater area overlap and superior performance.

1) *Poor improvement stroke patient*: Fig. 9 illustrates the performance evaluation for poor improvement stroke patient using AO, FPR, FNR and DC. According to the findings, the adaptive threshold technique outperforms other segmentation methods, demonstrating superior results. Specifically, the adaptive threshold technique exhibits high AO and DC along with low FPR and FNR outcomes.

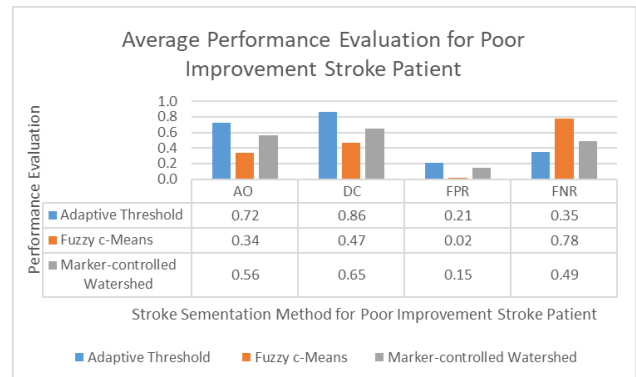


Fig. 9. Average performance evaluation for poor improvement stroke patient.

The adaptive threshold technique yields values of 0.72 for AO and 0.86 for DC. FPR signifies errors related to over-segmentation, while FNR denotes errors linked to under-segmentation. Lower values for both FPR and FNR are desired to minimize errors. The outcomes reveal that the adaptive threshold segmentation technique effectively distinguishes hyperintense lesions from other intensity pixels in the SWI image, displaying a low FPR of 0.21 and a low FNR of 0.35. For poor improvement stroke patients, the FCM technique stands out with the best FNR value, indicating no over-segmentation errors. In contrast, the marker-controlled watershed technique exhibits a high FNR for poor improvement stroke patients.

2) *Moderate improvement stroke patient*: In Fig. 10, the performance evaluation for moderate improvement stroke patient using AO, FPR, FNR and DC. According to the

findings, the adaptive threshold technique again stands out as the superior segmentation method among others.

The adaptive threshold technique demonstrates favorable outcomes with high AO and DC values along with low FPR and FNR results. Specifically, the AO and DC values achieved by the adaptive threshold technique are 0.83 and 0.94, respectively. The findings indicate that this segmentation method effectively distinguishes hyperintense lesions from other intensity pixels in the SWI image, displaying a low FPR of 0.15 and a low FNR of 0.29. The adaptive threshold technique attains the best under-segmentation rate compared to other techniques. However, the FCM technique achieves the best FNR result, recording 0.87.

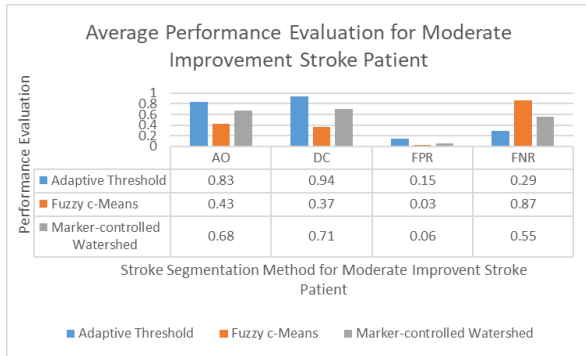


Fig. 10. Average performance evaluation for moderate improvement stroke patient.

3) *Good improvement stroke patient*: Fig. 11 determines the performance evaluation for good improvement stroke patient using AO, FPR, FNR and DC. According to the results, the adaptive threshold technique once again emerges as the leading segmentation method among others.

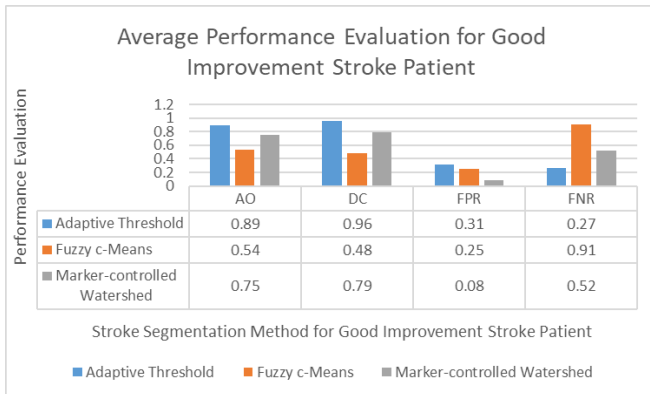


Fig. 11. Average performance evaluation for good improvement stroke patient.

The adaptive threshold technique exhibits high AO and DC values with low FPR and FNR outcomes. Specifically, the AO and DC values attained by the adaptive threshold technique are 0.89 and 0.96, respectively. The least favorable over-segmentation result is observed in FCM for stroke patients with significant improvement, featuring an FPR error of 0.08. In contrast, the adaptive threshold technique achieves the best FPR value at 0.31, indicating its efficacy in segmenting hypointense lesions with minimal over-segmentation error.

However, the FCM technique records the best value for FNR error, standing at 0.1.

D. Comparison Result of Performance Verification for the Stroke Lesion Classification Benchmarking

Based on previous research, Table V concluded the results by other researchers in similar studies. The Adaptive threshold segmentation technique has shown best dice coefficient compare to other studies. The dice coefficient value obtain was 0.97. Tetteh et al. (2023) presents dice coefficient value with 0.76% by using Marker-Controlled Watershed. Kuang et al. (2023) presents the second highest dice coefficient value with 0.89. Rava et al. (2021) presents dice coefficient value with 0.83. Gong et al. (2021) dice coefficient value with 0.87. At last, Su et al. (2020) presents dice coefficient value 0.75.

TABLE V. MACHINE LEARNING TECHNIQUE FOR BRAIN STROKE DIAGNOSIS BY OTHER RESEARCHERS

Author	Imaging Modality	Number of Data	Technique	Result
Proposed method	MRI	24 patients	Adaptive Threshold	0.96
Tetteh et al. (2023, [27])	MRI	183 patients	Marker-Controlled Watershed	0.76
Kuang et al. (2023, [28])	CT	154 patients	Adaptive Threshold	0.89
Rava et al. (2021, [29])	CBCT	200 patients	k-Means	0.83
Hokkinen et al. (2021, [30])	MRI	89 patients	Adaptive Threshold	0.97
Gong et al. (2021, [31])	CT	30 patients	Fuzzy Means (FCM)	0.87
Su et al. (2020, [32])	MRI	269 patients	Region Growing	0.75

V. CONCLUSION

In this research, machine learning techniques are proposed for automatic scoring of brain stroke diagnosis in the context of treatment decision making in ischemic stroke. The automated technique to locate, segment and quantify the lesion area would support clinicians and neuroradiologists rendering their findings more robust and reproducible. The techniques are highly capable to classify the type of brain stroke and accurate diagnosis for ischemic stroke patient into two types, those are stable and worse stroke patient. The outcome of this research could serve as an insight to improve the healthcare of the community by providing better solutions using such intelligent system. Furthermore, the characteristics of stroke lesion appearances, their evolution, and the observed challenges should be study in detail.

ACKNOWLEDGMENT

The study is funding by Ministry of Higher Education (MOHE) of Malaysia through the Fundamental Research Grant Scheme (FRGS), No: FRGS/1/2022/SKK06/UTEM/02/1). The authors also would like to thank Faculty of Electrical Engineering, Universiti Teknikal Malaysia Melaka (UTeM)

and to all team members of Advanced Digital Signal Processing Group (ADSP), Centre of Robotic & Industrial Information (CeRIA), for their contribution and suggestion to successfully complete this paper.

REFERENCES

- [1] J. E. Son, D. S. Chow, and M. Nagamine, "Artificial intelligence and acute stroke imaging," *AJNR. American Journal of Neuroradiology*, vol. 42, no. 1, 2021.
- [2] A. K. Boehme, C. Esenwa, and M. S. V. Elkind, "Stroke Risk Factors, Genetics, and Prevention," *Cross Ref Medline*, vol. 120, no. 3, pp. 472–495, 2017.
- [3] E. J. Lee, Y. H. Kim, N. Kim, and D. W. Kang, "Deep into the brain: artificial intelligence in stroke imaging," *Journal of Stroke*, vol. 19, no. 3, pp. 277–285, 2017.
- [4] A. A. Valliani, D. Ranti, and E. K. Oermann, "Machine learning and neurology: a systematic review," *Neurology and Therapy*, vol. 8, no. 2, pp. 351–365, 2019.
- [5] N. M. Murray, M. Unberath, G. D. Hager, and F. K. Hui, "Artificial intelligence to diagnose ischemic stroke and identify large vessel occlusions: a systematic review," *Journal of Neurointerventional Surgery*, vol. 12, no. 2, pp. 156–164, 2020.
- [6] H. Kamal, V. Lopez, and S. Sheth, "Machine learning in acute ischemic stroke neuroimaging," *Frontiers in Neurology*, vol. 9, no. 2018, p. 945, 2018.
- [7] C. Krittanawong, H. J. Zhang, Z. Wang, M. Aydar, and T. Kitai, "Artificial intelligence in precision cardiovascular medicine," *Journal of the American College of Cardiology*, vol. 69, no. 21, pp. 2657–2664, 2017.
- [8] P. Xanthopoulos, P. M. Pardalos, T. B. Trafalis, P. Xanthopoulos, P. M. Pardalos, and T. B. Trafalis, "Linear discriminant analysis," in *Robust Data Mining*, pp. 27–33, Springer, New York, NY, 2013.
- [9] S. Castaneda-Vega, P. Katiyar, F. Russo et al., "Machine learning identifies stroke features between species," *Therapeutics*, vol. 11, no. 6, pp. 3017–3034, 2021.
- [10] M. Bento, R. Souza, M. Salluzzi, L. Rittner, Y. Zhang, and R. Frayne, "Automatic identification of atherosclerosis subjects in a heterogeneous MR brain imaging data set," *Magnetic Resonance Imaging*, vol. 62, pp. 18–27, 2019.
- [11] J. Vargas, A. Spiotta, and A. R. Chatterjee, "Initial experiences with artificial neural networks in the detection of computed tomography perfusion deficits," *World Neurosurgery*, vol. 124, pp. e10–e16, 2019.
- [12] M. S. Sirsat, E. Fermé, and J. Cmara, "Machine learning for brain stroke: a review. Science Direct," *Journal of Stroke and Cerebrovascular Diseases*, vol. 29, no. 10, 2020.
- [13] S. A. Sheth, L. Giancardo, M. Colasurdo, V. M. Srinivasan, A. Niktabe, and P. Kan, "Machine learning and acute stroke imaging," *Journal of Neurointerventional Surgery*, p. neurint-surg-2021-018142, 2022.
- [14] H. P. Chan, R. K. Samala, L. M. Hadjiiski, and C. Zhou, "Machine learning in medical image analysis," *Medical Image Analysis*, vol. 1213, 2020.
- [15] M. Puttagunta and S. Ravi, "Medical image analysis based on machine learning approach," *Multimedia Tools and Applications*, vol. 80, no. 16, pp. 24365–24398, 2021.
- [16] J. Zhang, Y. Xie, Q. Wu, and Y. Xia, "Medical image classification using synergic machine learning," *Medical Image Analysis*, vol. 54, pp. 10–19, 2019.
- [17] H. J. Van Os, L. A. Ramos, A. Hilbert et al., "Predicting outcome of endovascular treatment for acute ischemic stroke: potential value of machine learning algorithms," *Frontiers in Neurology*, vol. 9, 2018.
- [18] L. Li, M. Wei, B. Liu et al., "Machine learning for hemorrhagic lesion detection and segmentation on brain MRI images," *IEEE Journal of Biomedical and Health Informatics*, vol. 25, no. 5, pp. 1646–1659, 2021.
- [19] S. Zhang, M. Zhang, S. Ma et al., "Research progress of machine learning in the diagnosis and prevention of stroke," *BioMed Research International*, vol. 2021, Article ID 5213550, 5 pages, 2021.
- [20] A. Krizhevsky, I. Sutskever, and G. E. Hinton, "Magenet classification with deep convolutional neural networks," in *Proc. Adv. Neural Inf. Process. Syst.*, pp. 1097–1105, Harrahs and Harveys, Lake Tahoe, 2012.
- [21] C. Szegedy, W. Liu, Y. Jia et al., "Going deeper with convolutions," in *Proc. IEEE Conf. Comput. Vis. Pattern Recognit.*, pp. 1–9, MA, USA, 2015.
- [22] R. Yang and Y. Yu, "Artificial convolutional neural network in object detection and semantic segmentation for medical imaging analysis," *Frontiers in Oncology*, vol. 11, p. 638182, 2021.
- [23] L. N. Do, B. H. Baek, S. K. Kim, H. J. Yang, I. Park, and W. Yoon, "Automatic assessment of aspects using diffusion-weighted imaging in acute ischemic stroke using recurrent residual convolutional neural network," *Diagnostics*, vol. 10, no. 10, p. 803, 2020.
- [24] G. B. Praveen, A. Agrawal, P. Sundaram, and S. Sardesai, "Ischemic stroke lesion segmentation using stacked sparse auto-encoder," *Computers in Biology and Medicine*, vol. 99, pp. 38–52, 2018.
- [25] A. Pinto, S. Pereira, R. Meier et al., "Combining unsupervised and supervised learning for predicting the final stroke lesion," *Medical Image Analysis*, vol. 69, p. 101888, 2021.
- [26] D. Shome, T. Kar, S. N. Mohanty et al., "COVID-transformer: interpretable covid-19 detection using vision transformer for healthcare," *International Journal of Environmental Research and Public Health*, vol. 18, no. 21, p. 11086, 2021.
- [27] G. Tetteh, F. Navarro, R. Meier, J. Kaesmacher, J.C. Paetzold, J.S. Kirschke, C. Zimmer, R. Wiest, and B.H. Menze, "A machine learning approach to predict collateral flow in stroke patients using radiomic features from perfusion images," *Frontiers in Neurology*, vol. 14, no. 1, 2023.
- [28] H. Kuang, W. Wan, Y. Wang, J. Wang, and W. Qiu, "Automated Collateral Scoring on CT Angiography of Patients with Acute Ischemic Stroke Using Hybrid CNN and Transformer Network," *Biomedicines*, vol. 11, no. 2, 2023.
- [29] R.A. Rava, S.E. Seymour, K.V. Snyder, M. Waqas, J.M. Davies, E.I. Levy, A.H. Siddiqui, and C.N. Ionita, "Automated Collateral Flow Assessment in Patients with Acute Ischemic Stroke Using Computed Tomography with Artificial Intelligence Algorithms," *World Neurosurgery*, vol. 155, pp. e748–e760, September 2021.
- [30] L. Hokkinen, T. Mäkelä, S. Savolainen, and M. Kangasniemi, "Computed tomography angiography-based machine learning method for treatment selection and infarct volume prediction in anterior cerebral circulation large vessel occlusion," *Acta Radiologica Open*, vol. 10, no. 11, p. 205846012110603, 2021.
- [31] Q. Gong, B. Yu, M. Wang, M. Chen, H. Xu, and J. Gao, "Predictive Value of CT Perfusion Imaging on the Basis of Automatic Segmentation Algorithm to Evaluate the Blood Flow Status on the Outcome of Reperfusion Therapy for Ischemic Stroke," *Journal of Healthcare Engineering*, 2021.
- [32] J. Su, L. Wolff, A.C.G.M. Es, W. Van Zwam, C. Majoie, D.W.J. Dippel, A. Van Der Lugt, W.J. Niessen, and T. Van Walsum, "Blood Flow MRI Images," *IEEE Transactions on Medical Imaging*, vol. 39, no. 6, pp. 2190–2200, 2020.